Magnetite Fe_3O_4 Nanocrystals: Spectroscopic Observation of Aqueous Oxidation Kinetics†

Jing Tang, Matt Myers,‡ Ken A. Bosnick, and Louis E. Brus*

Department of Chemistry, Columbia University, New York, New York 10027

Received: September 22, 2002

Low-temperature oxidation of aqueous magnetite nanoparticles to maghemite has been monitored via the loss of near-IR optical absorbance. The kinetics closely follows the diffusion in a sphere model as suggested by previous literature reports. The temperature dependence of the diffusion constant is described by an Arrhenius equation with an activation energy of 21.0 kcal/mol. No intermediate optical spectra are observed, which confirms the extremely local nature of the optical transitions. A careful search for photooxidation establishes a small upper limit for the possible increase in the diffusion constant under illumination.

Introduction

Magnetite (Fe_3O_4) and maghemite (γ-Fe_2O_3) are widespread in the environment, despite the fact that both are thermodynamically unstable with respect to hematite (α-Fe_2O_3) in the presence of oxygen. They are found in bacteria and insects, weathered soils and clays, rocks, natural-atmospheric and polluted aerosols, and even on the surface of Mars.[1] Near room temperature, magnetite very slowly oxidizes to maghemite, and then at higher temperatures, to hematite. The oxidation of magnetite to maghemite is thus a significant environmental process, and in this paper we study the optical spectroscopy and oxidation kinetics of aqueous colloidal 9-nm nanocrystals. Magnetite and maghemite nanoparticles are also widely used as ferrofluids[2] such as in rotary shaft sealing, dynamic loudspeakers, and computer hard drives, and also have medical use in, for example, magnetic resonant imaging and targeted drug transportation.

Magnetite is a spin-polarized, $Fe^{2+}-Fe^{3+}$ mixed-valence metal with a DC conductivity at 23 °C of about 0.1% that of Cu metal. Its crystals appear black and absorb throughout the UV-vis-IR spectrum. Maghemite, by contrast, is an insulator with a ca. 2 eV optical absorption threshold. Both phases are ferrimagnetic and have an inverse spinel oxygen lattice with almost identical unit cell dimensions. Magnetite undergoes a metal−insulator phase transition below about 120 K in which the conductivity abruptly decreases by a factor of ∼100.[3] This Verwey transition has been modeled as charge ordering, but remains poorly understood and is the subject of much current research. At 23 °C, electrical transport is thought to occur via thermally activated polaronic hopping of Fermi surface electrons from Fe ion to Fe ion in octahedral sites. Band structure calculations indicate that the strong internal magnetic field splits the narrow Fe d electron bands into separate spin-up and spin-down bands; the lower band in octahedral sites is partially filled as shown in Figure 1a. Thus magnetite is a spin-polarized metal. There is weak Marcus-type electron localization into a polaron due to the movement of oxygen nuclei around the initially delocalized metallic d electrons. This localization creates a temperature-dependent intervalence charge transfer (IVCT) absorption band in the IR at 0.6 eV (see Figure 1b).[4−5] We monitor this band as the oxidation process proceeds.

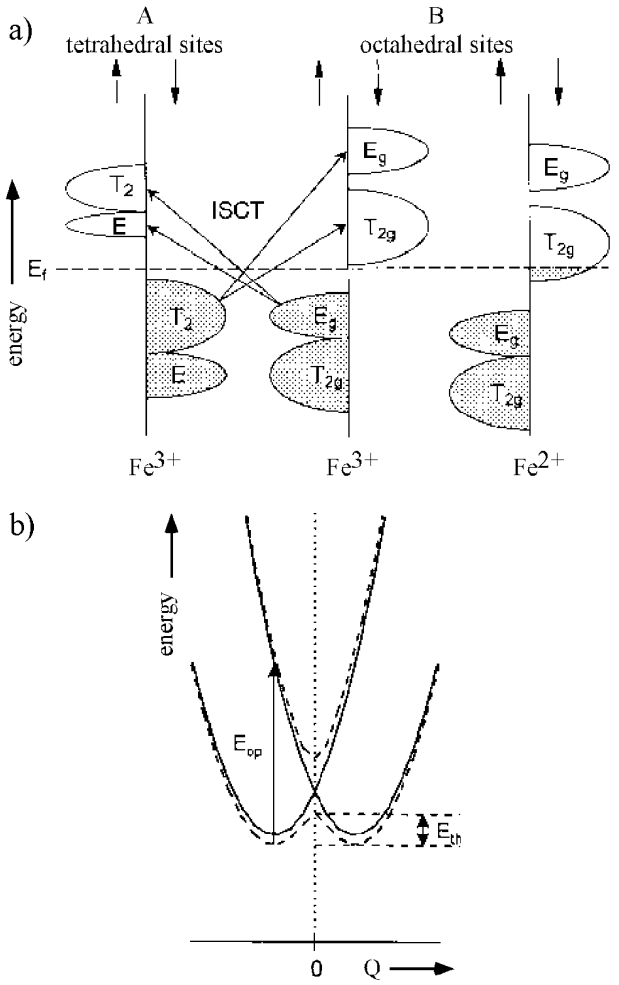

Figure 1. (a) Schematic representation of the electron energy levels of the Fe ions in Fe_3O_4. (b) Simplified diagrams of potential energy versus configuration coordinate for two equivalent sites. The dotted line represents the potential energy for the case of a partly delocalized electron. E_{op} and E_{th} represent optical and thermal energy, respectively (adapted from ref 4).

Most prior oxidation studies have been done on larger dry magnetite particles in air, using X-ray diffraction and/or

† Part of the special issue "Arnim Henglein Festschrift".

* Author to whom correspondence should be addressed. E-mail: brus@chem.columbia.edu.

‡ REU student from Department of Chemical Engineering, California Institute of Technology.

10.1021/jp027048e CCC: $25.00
Published on Web 04/16/2003

chemical analysis methods. Oxidation is believed to occur through the outward diffusion of iron cations.[6−10] Gallagher et al. calculated the distribution of Fe^{2+} across magnetite particles after different degrees of oxidation.[6] Sidhu et al. directly demonstrated that the concentration of Fe^{2+} decreases from the center to the surface of the particles as oxidation proceeds, by dissolving the partially oxidized particles in very dilute HCl.[8] They also found that when heating at 220 °C magnetite crystals that were synthetically substituted with trace elements (Co, Ni, Zn, Cu, Mn, and Cr), the outer regions of the oxidized particles contained less of these elements, which again indicates an outward movement of Fe during the transformation.[9] Presumably, at the surface the Fe reacts with O_2 and forms a thin layer of epitaxial maghemite.

In this paper, we study the oxidation of magnetite nanoparticles to maghemite in aqueous solution via the loss of near-IR absorption. The kinetics does not fit simple rate-laws, but rather fits the diffusion in a sphere model used by Sidhu et al. for dry oxidation.[8] The Fe diffusion constants and the activation energy in water agree well with the values reported for dry oxidation of larger particles. In addition to the thermal oxidation, photo effects on the oxidation were also studied.

Experiment

Synthesis of Magnetite Nanoparticles. Magnetite nanoparticles were synthesized by chemical coprecipitation of $FeCl_3$ and $FeCl_2$ in an alkaline medium.[11] Amounts of 0.324 g $FeCl_3$ (2 mmol) and 0.127 g $FeCl_2$ (1 mmol) were dissolved in 10 mL of deoxygenated water and then added dropwise to 8 mL of 1 M deoxygenated tetramethylammonium hydroxide (TMAOH) in water under vigorous stirring with the protection of nitrogen. A black precipitate instantly formed. After stirring for 30 min, the magnetite precipitate was washed three times with distilled water by magnetic decanting. The final product was then redissolved in 1 M aqueous TMAOH and formed a stable colloid solution. Due to the strong magnetic dipole−dipole interactions between the particles as well as the high surface energy of magnetic metal oxide surfaces, magnetite particles tend to agglomerate and TMAOH was used instead of NH_4OH or NaOH as TMAOH serves not only as the basic reactant, but also leads to an electric double layer stabilization in aqueous media.[12−13]

Characterizations of the Synthesized Magnetite Nanoparticles and Their Oxidized Products. Both materials were characterized by transmission electron microscopy (TEM), electron diffraction, atomic force microscopy (AFM), and Raman scattering. TEM images were taken with a Phillips Electron Transmission Microscope EM430 at 300 kV with samples made by dropping the solutions on formvar-coated grids (Ted Pella F-01409). To take the Raman spectra, a paste of the particles was deposited on a quartz coverslip, and the Raman was excited with ∼2.5 mW of 632 nm light from a He−Ne laser focused to a spot of ∼1 μm^2.

Oxidation. The magnetite solution was diluted with distilled water by a factor of ∼20−40, resulting in a ∼2 mM solution (in Fe_3O_4 formula units) with a pH of 12−13. Except for the room-temperature experiment, the solution was then heated in air under reflux (to prevent the loss of the solvent which would lead to change in the concentration of the solution) with a thermocouple immersed in the solution to monitor the temperature directly. Aliquots of solution were taken out after certain periods of time and cooled immediately with ice water to quench the reaction. UV−vis−near-IR spectra of the solutions were taken using a Perkin-Elmer Lambda 19 instrument. Due to the absorption of water in the near-IR region, the spectra are taken to 1350 nm in a 1 cm optical path cuvette (NIR quartz, Spectracell) and to 1800 nm in a 1 mm optical path cuvette (NIR quartz, Spectracell).

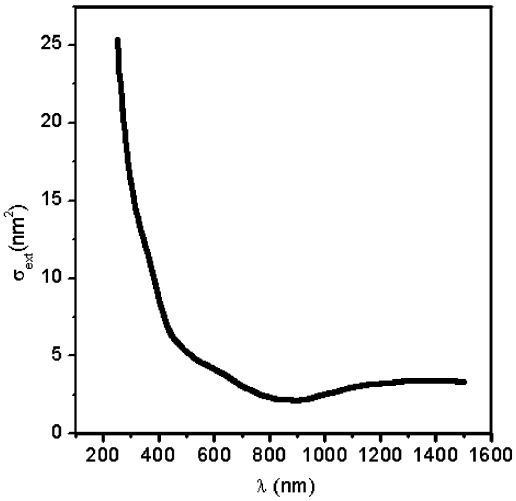

Figure 2. Extinction cross section (σ_{ext}) of 10 nm diameter magnetite particles in water calculated using Mie theory. The calculations predict that magnetite particles have an absorption band in the near-IR.

Results and Discussions

Mixed valence iron oxides and silicates, including magnetite, exhibit thermally induced electron delocalization between adjacent Fe^{2+} and Fe^{3+} ions, and electronic transitions assigned to intervalence charge transfer (IVCT) transitions in the visible and near-IR region. Fontijn et al. measured both the optical and the magnetooptical polar Kerr spectra of pure, Mg^{2+}-substituted, and Al^{3+}-substituted Fe_3O_4 crystals at 293 K, and the observed trends in the major transitions upon substitution are indicative of IVCT transitions occurring at 0.56, 1.94, 3.11, and 3.94 eV.[14] Strens et al. measured diffuse reflectance spectra of various iron oxides and only the spectra of magnetite and wustite (FeO) show finite absorption in the near-IR region while spectra of other iron oxides, e.g, maghemite, show almost no absorption beyond ∼700 nm.[15] Sherman et al. studied maghemite particles produced by oxidizing magnetite.[16] The diffuse reflectance of maghemite particles in the near-IR region increases as the degree of oxidation of the particles increases.

In our clear, nonscattering, stabilized colloids the optical extinction spectra should reflect the properties of individual particles. We did Mie scattering calculations for magnetite particles small compared with the wavelength[17] using the refractive indices from ref 14. As shown in Figure 2, the extinction spectrum of 10 nm diameter magnetite particles shows the near-infrared charge-transfer band. The calculation also shows that the absorption dominates over the scattering for 10 nm particles. As an insulator maghemite should have no absorption in the near-IR region; however, we could not find accurate dielectric data for Mie calculations on maghemite. From these experimental studies and calculations, we expect the absorption in the near-IR to decrease as magnetite is oxidized to maghemite. This is confirmed by our experiments.

TEM images (see for example Figure 3) show that the synthesized magnetite particles are mostly spherical and the size distribution of the particles is 8.7 ± 1.6 nm in diameter. Although the electron diffraction pattern can hardly distinguish between magnetite and maghemite, as these two phases have

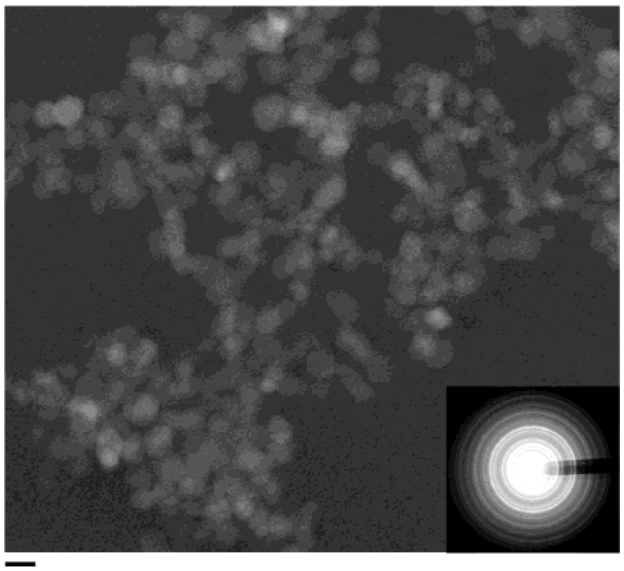

Figure 3. Representative TEM image of the synthesized magnetite nanoparticles. The scale bar is 10 nm. The inset in the lower right corner is the electron diffraction pattern of the particles. The average size of the particles is 8.7 nm.

very minor difference in diffraction (electron or X-ray) due to their identical crystal structures, it shows that the particles are highly crystalline. However, the two phases have very distinct bulk Raman spectra,[18−19] and this was used to determine the phase of the particles. The magnetite nanoparticles show the diagnostic Raman peak at ~672 cm^{-1}, which is consistent with the results of bulk phases in the literature.

When the magnetite solution was heated under air the color progressively changed from black to orange-red. As shown in Figure 4, the absorption of the magnetite in the near-IR region decreased and became flat after about 3 h at 80 °C. There was no change in the spectrum if the heated magnetite solution was continuously deoxygenated by bubbling nitrogen through it under otherwise identical conditions. The dissolved oxygen concentration in water at room temperature corresponds to a pressure of 4.5 Torr[20] and decreases slowly with increasing temperature. The final orange-red particles move when a magnet is brought close to them (after evaporating some of the solvent and precipitating the particles), indicating that they have not been oxidized to hematite. They are further confirmed to be maghemite nanoparticles by their Raman spectrum which shows three broad peaks at around 680, 500, and 380 cm^{-1}, similar to the bulk spectra reported in the literature. TEM or AFM images show no significant change in either the shape or average size of the particles. This is consistent with previous literature reports[6,21−22] indicating that the oxidation process of magnetite to maghemite by heating is a topotactic reaction in which the original particle morphology is maintained throughout.

The optical spectra in the 1 mm optical path cuvette show an unambiguous isobestic point in the visible at ~400 nm. This suggests that only two spectra are present in various proportions as the reaction proceeds. When the spectra of the initial magnetite and final maghemite are superimposed with the corresponding conversion ratio, the resulting spectra closely fit the partially oxidized spectra, for example, as shown in Figure 5 for the 30 min intermediate during the 80 °C oxidation. This indicates that from the optical point of view, no intermediate species form during the process of oxidation. Yet, from the prior results we know there is a continuous range of stoichiometries present during oxidation; note also that the two phases can form

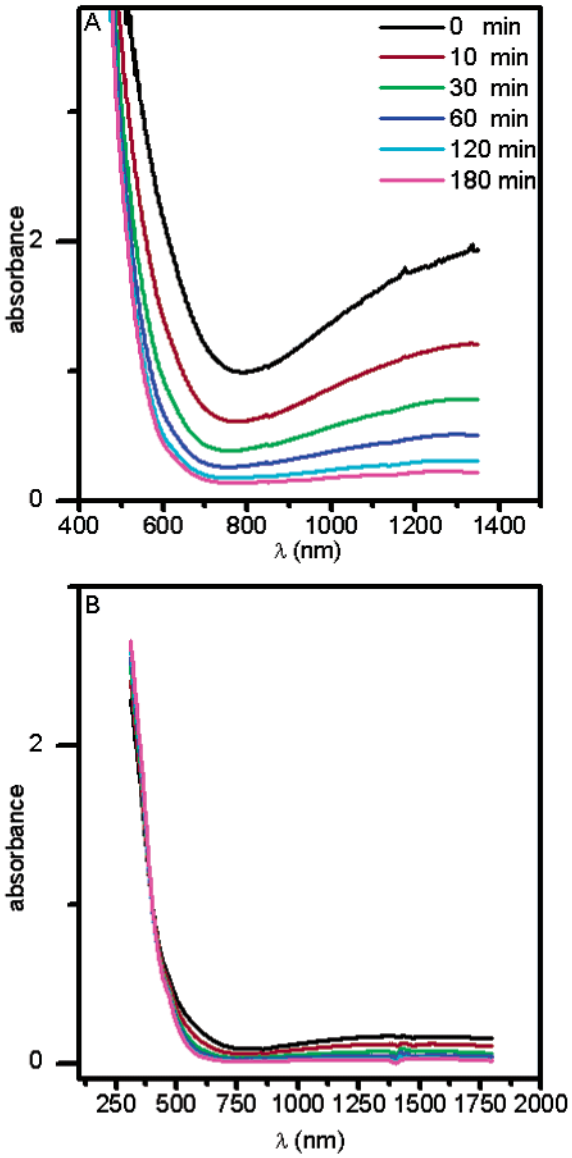

Figure 4. The change of the UV−vis−NIR absorption spectra as magnetite nanoparticles oxidize to maghemite at 80 °C. Spectra in 4A were taken with a 1 cm optical path, while those in 4B were taken with a 1 mm optical path. From top to bottom, the spectra correspond to reaction times of 0, 10, 30, 60, 120, and 180 min.

a complete solid solution series.[22−24] This observation confirms the extreme localized nature of the optical spectra in these materials, in contrast with the spectra of a delocalized semiconductor, for example. Loosely speaking, in the IR charge-transfer absorption of one Fe^{2+}, it does not matter how many other Fe^{2+} ions are in the local neighborhood. Also, the Fe^{3+} transitions in the UV−vis have essentially the same spectrum in the presence or absence of nearby Fe^{2+}.

From the decrease of the absorption in the near-IR region, the conversion fraction of magnetite to maghemite (i.e., Fe^{2+} to Fe^{3+}) can be calculated. For example, Figure 6 shows the change in Fe^{2+} content in percentage (denoted by α) and ln α as a function of reaction time during oxidation at 50 °C. Noticeably, the reaction is relatively fast at the beginning and slow toward the end, and the kinetics does not fit simple rate laws. Our experiments also found that the reaction rate depends very strongly on the temperature; the time needed for reaction to near completion varies from 3 h at 80 °C to about three months at room temperature.

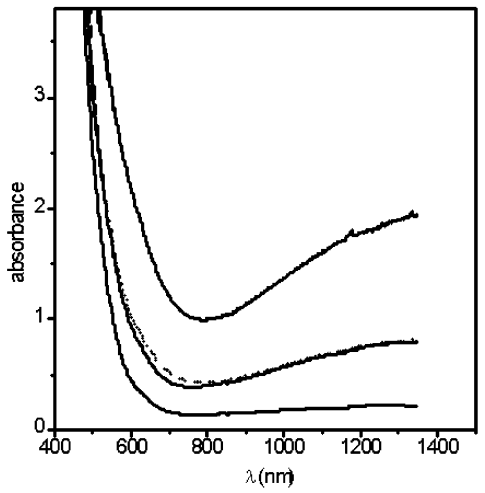

Figure 5. The solid lines, from the top to bottom, correspond to absorption spectra of the initial magnetite solution, the solution after 30 min oxidation, and the final maghemite solution. The dashed line is a superposition of the spectra from the initial and final solutions with weights corresponding to the 30 min conversion, showing that there are no obvious intermediates.

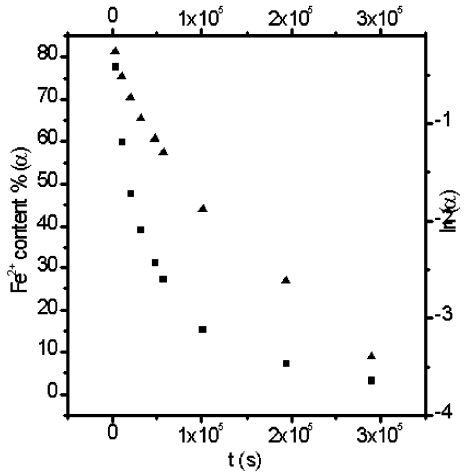

Figure 6. Kinetic plot of the oxidation at 50 °C. The squares shows the change in Fe^{2+} content in percentage (denoted by α, left *y*-axis) as a function of reaction time. The triangles indicate ln α (right *y*-axis) as a function of time.

TABLE 1: Calculated Iron Diffusion Constants and Half Lives ($t_{1/2}$) at Different Temperatures ($D^a$and $D^b$are diffusion constants derived from the slope and intercept of eq 3, respectively.)

T (°C)	24	50	65	80
D^a (10^{-20} cm^2/s)	1.13	26.7	96.9	595
D^b (10^{-20} cm^2/s)	1.50	24.3	88.1	561
$t_{1/2}$ (min)	9760	338	94	15

As previously indicated, prior dry studies suggest that the oxidation occurs through the outward diffusion of iron cations. As our magnetite particles are spherical and the size change after oxidation is negligible, we followed the diffusion in a sphere model of Sidhu et al.[8] The diffusion of noninteracting particles in a sphere[25] can be represented by

$$\frac{\partial C}{\partial t} = D\left(\frac{\partial^2 C}{\partial r^2} + \frac{2}{r}\frac{\partial C}{\partial r}\right) \tag{1}$$

where *D* is the diffusion constant, *C* is the concentration of the iron species to be oxidized, and *r* is the radial position. With the assumptions that Fe^{2+} is immediately oxidized once it gets to the surface so that $C = 0$ at the surface, the fractional conversion is found to be described by

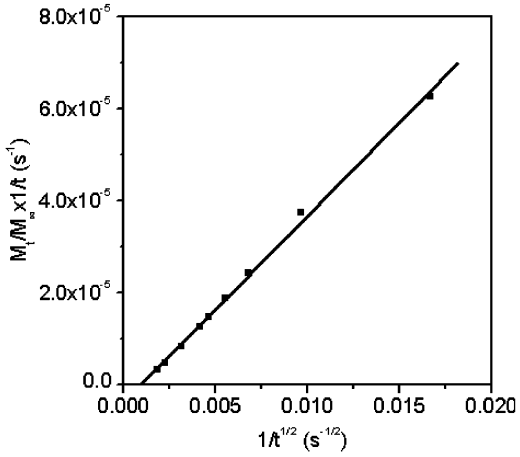

Figure 7. $(M_t/M_\infty) \times 1/t$ vs $t^{-1/2}$ plot of the data on oxidation of magnetite particles at 50 °C. The Fe diffusion constants were derived from both the slope and intercept.

$$\frac{M_t}{M_\infty} = 6\pi^{-1/2}\left(\frac{Dt}{a^2}\right)^{1/2} - 3\frac{Dt}{a^2} \tag{2}$$

where M_t is the quantity of Fe that has diffused out after time *t* and M_∞ is the corresponding quantity after infinite time. Dividing each side by *t*, we get

$$\frac{M_t}{M_\infty} \times \frac{1}{t} = 6\pi^{-1/2}\left(\frac{D}{a^2}\right)^{1/2} \times \frac{1}{t^{1/2}} - 3\frac{D}{a^2} \tag{3}$$

Therefore, a plot of $(M_t/M_\infty)/t$ versus $t^{-1/2}$ should give a straight line. The diffusion constant is obtained from either the slope or the intercept if the sphere radius is known.

Equation 3 fits our kinetic data (at four different temperatures) very well. (The data for 50 °C is shown in Figure 7.) The diffusion constants obtained from the slope and the intercept are quite close as listed in Table 1. The average size obtained from TEM is used for the radius of the particles. The effect of temperature on the diffusion coefficients is described using an Arrhenius type equation

$$D = D_0 \exp(-E/RT) \tag{4}$$

where *E* is the activation energy, *R* is the gas constant, *T* is the absolute temperature, and D_0 is the frequency factor. The activation energy calculated from the plot of ln *D* vs 1/*T* (Figure 8) is 21.0 kcal/mol, which is very close to the value Sidhu[8] obtained of 19.4 kcal/mol as well as that of 20 ± 2 kcal/mol obtained by Colombo.[26] The frequency factor D_0 is found to be 7.2×10^{-5} cm^2/s and is similar to the reported value 3.16×10^{-5} cm^2/s. Sidhu also compared the frequency factor with the theoretical value for crystalline solid according to the theory of rate processes.[8,27] Theoretically, the frequency factor will be $d\upsilon/3$, where *d* is the distance between the nearest neighbors in the lattice and υ is the mean molecular velocity. For magnetite, it is calculated to be 2.05×10^{-4} cm^2/s, which is close to our experimentally determined value.

With our values of D_0 and *E* and eq 4, the diffusion constants at temperatures of 190−210 °C can be predicted and agree well with the diffusion constants Sidhu obtained at the corresponding temperatures. However, both their and our diffusion constants are about 12 orders of magnitude lower than the values

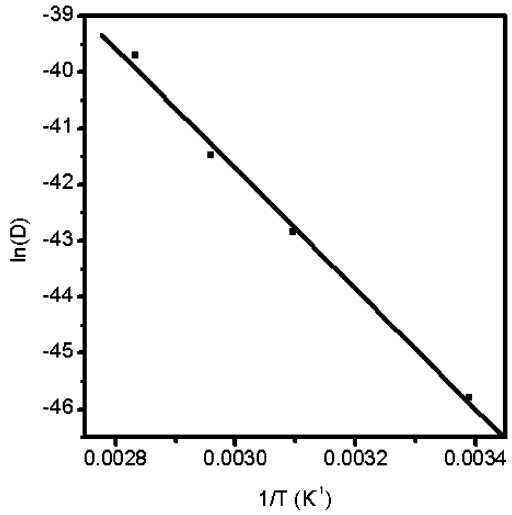

Figure 8. Arrhenius plot of the Fe diffusion coefficients. E and D_0 are determined to be 21.0 kcal/mol and 7.2×10^{-5} cm^2/s, respectively.

Gallagher reported, and as argued by Sidhu, the diffusion constants calculated by Gallagher appear to be too large for a diffusion process in the solid phase.

The diffusion mechanism predicts that the oxidation time will be strongly dependent on the size of the crystal; in small crystals the diffusion lengths are short. Although we have not made stable solutions of magnetite of different sizes, comparisons with the larger particles studied in previous papers indicate that our results qualitatively agree with this predicted sized dependence. The temperatures needed for the oxidation of nanoparticles to occur in a few hours are much lower than those used in studies of larger particles, which are usually above 150 °C. At room temperature, the oxidization rate of our nanocrystals is much faster than that of the bigger particles. Murad et al. reported that it took years for the ultra fine magnetite crystals (100−300 nm) to change to maghemite at room temperature;[28] in Sidhu's paper, the particle size used was a couple of hundred nanometers and oxidation did not occur after one year. Our experiment shows that for 9 nm nanocrystals at 24 °C in water, oxidation is detectable after a few hours and completed in about three months.

Our experiments do not determine what species is diffusing. Oxidation from magnetite to maghemite involves a reduction in the number of Fe atoms per unit cell, from 24 in magnetite to $21^1/_3$ in maghemite. The inverse spinel structure is maintained during oxidation and therefore the oxygen arrangement does not change. These facts favor the diffusion of Fe outward over the diffusion of oxygen inward. Moreover, an oxygen ion is almost twice as big as an iron ion and this would make the oxygen diffusion much harder compared to iron diffusion. Studies on the cation self-diffusion of magnetite[29] show that the Fe^{2+} ions are mainly responsible for diffusion.

As oxidation proceeds prior results indicate there is no sharp interface between magnetite and maghemite phases in each particle, as would occur in the oxidation of Si particles to SiO_2 for example. As the local stoichiometry continuously changes, local electrical neutrality must be preserved. Fe atoms diffusing to the surface must be screened to appear neutral on some length scale by the metallic electrons, which move with the Fe atom. In the beginning of the process, the Fe atoms are diffusing in an effectively metallic Fe_3O_4 lattice, while near the end the Fe atoms are diffusing in an effectively insulating Fe_2O_3 lattice. It is surprising that a model of noninteracting particles with diffusion constant D independent of local stoichiometry fits the data well. Perhaps this is a consequence of the fact that the oxygen inverse spinel lattice and thus the octahedral and tetrahedral Fe sites change so little during oxidation.

In addition to thermal oxidation, we have studied possible photooxidation of magnetite. Iron oxides exist on the surface of Mars, and it has been postulated that light may play a role in the transformation of magnetite to maghemite or hematite. Huguenin studied the kinetics of the photostimulated oxidation of magnetite and claimed that magnetite oxidizes directly to hematite upon exposure to UV and visible light.[30−31] Morris et al. disputed Huguenin's conclusion and concluded that there was no perceptible UV photo stimulated oxidation for a variety of particulate magnetites.[32] However, in both papers, high power lamps which heat the sample have been used as light sources. As temperature has a huge effect on this oxidation process, it is difficult to separate the thermal effect from the photo effect. In our experiments, great care has been taken to achieve this separation. A 300 W quartz-tungsten lamp was used to study the effect of visible and near-IR light. Although the reaction container was kept cool in an ice−water bath, the temperature of the solution would still be around 25 °C as a result of the heating effect of the lamp. Compared with the data we already obtained at room temperature, we conclude that visible light has no effect on the oxidation.

For the ultraviolet source we used a 100 mW multi-line UV argon laser (334−364 nm) as the light source. Our experimental configuration had a long enough path length that virtually all of the incident photons ($\sim 10^{17}$ s^{-1}) were absorbed by the particles. We estimate the number of particles to be $\sim 10^{15}$ from the measured extinction spectrum and the calculated extinction cross section per particle. This gives $\sim 10^2$ photons absorbed per particle per second on average. A flowing water cooling system was used to keep the temperature constant (around 0 °C) under the laser illumination. A control experiment was done at the same temperature in the dark. It is found that there is a slight increase in the oxidation rate with the laser which is equivalent to about a 7 °C temperature increase predicted from our Arrhenius eq 4. That is, the diffusion constant at 0 °C is 6.3×10^{-22} cm^2/s while at 7 °C it is 1.6×10^{-21} cm^2/s. As an upper limit, the possible true increase in diffusion constant due to absorption of $\sim 10^2$ photons per second per particle is 9.7×10^{-22} cm^2/s. This might represent particle heating by the laser or a photo effect.

Conclusions

In summary, the oxidation of magnetite to maghemite has been studied in solution via the loss of optical absorption in the near-IR region. Consistent with previous reports for dry oxidation of larger particles, the oxidation is controlled by diffusion and fits the model of Sidhu et al. The diffusion coefficients and the activation energy were calculated and agree quantitatively with previous literature. The photo effect on the oxidation has also been carefully studied and we conclude that light has a very small effect on the oxidation process.

Acknowledgment. We greatly thank Franz Redl of IBM for taking the TEM images and Michael Steigerwald for helpful discussions. This work has been supported by the NSF via the Environment Molecular Sciences Institute (CHE-98-10367) and the MRSEC Program (DMR-0213574) at Columbia University.

References and Notes

(1) Cornell, R. M.; Schwertmann, U. *Iron Oxides Structure, Properties, Reactions, Occurrence and Uses*; VCH: Weinheim, 1996.

(2) Raj, K.; Moskowitz, R. J. *J. Magn. Magn. Mater.* **1990**, *85*, 233.
(3) Verwey, E. J. W. *Nature* **1939**, *144*, 327.
(4) Fontijn, W. F. J.; van der Zaag, P. J.; Feiner, L. F. *J. Appl. Phys.* **1999**, *85*, 5100.
(5) Park, S.; Ishikawa, T.; Tokura, Y. *Phys. Rev. B* **1998**, *58*, 3717.
(6) Gallagher, K. J.; Feitknecht, W.; Mannweler, U. *Nature* **1968**, *217*, 1118.
(7) Colombo, U.; Fagherazzi, G.; Gazzarrini, F.; Lanzavecchia, G.; Sironi, G. *Nature* **1968**, *219*, 1036; ibid. *Nature* **1964**, *202*, 175; ibid. *Science* **1965**, *147*, 1033.
(8) Sidhu, P. S.; Gilkes, R. J.; Posner, A. M. *J. Inorg. Nucl. Chem.* **1977**, *39*, 1953.
(9) Sidhu, P. S.; Gilkes, R. J.; Posner, A. M. *Soil Sci. Soc. Am. J.* **1980**, *44*, 135.
(10) Swaddle, T. W.; Oltmann, P. *Can. J. Chem.* **1980**, *58*, 1763.
(11) Kang, Y. S.; Risbud, S.; Rabolt, J. F.; Stroeve, P. *Chem. Mater.* **1996**, *8*, 2209.
(12) Babes, L.; Tanguy, D. G.; Jeune, J. J. L.; Jallet, P. *J. Colloid Interface Sci.* **1999**, *212*, 474.
(13) Berger, P.; Adelman, N. B.; Beckman, K. J.; Campbell, D. J.; Ellis, A. B.; Lisensky, G. *J. Chem. Educ.* **1999**, *76*, 943.
(14) Fontijin, W. F. J.; van der Zaag, P. J.; Devillers, M. A. C.; Brabers, V. A. M.; Metselaar, R. *Phys. Rev. B* **1997**, *56*, 5432.
(15) Strens, R. G. J.; Wood, B. J. *Miner. Magn.* **1979**, *43*, 347.
(16) Sherman, D. M.; Burns, R. G.; Burns, V. M. *J. Geophys. Res.* **1982**, *87*, 10169.
(17) Bohren, C. F.; Huffman, D. R. *Absorption and Scattering of Light by Small Particles*; John Wiley: New York, 1998.
(18) de Faria, D. L. A.; Venâncio Silva, S.; de Oliveira, M. T. *J. Raman Spectrosc.* **1998**, *28*, 873.
(19) Thibeau, R. J.; Brown, C. W.; Heidersbach, R. H. *Appl. Spectrosc.* **1978**, *2*, 532.
(20) Vesilind, P. A. *Introduction to Environmental Engineering*; PWS Publishing Company: Boston, 1996.
(21) Fietknecht, W.; Lehman, H. W. *Helv. Chim. Acta* **1959**, *42*, 2035.
(22) Fietknecht, W. *Mem. Sci. Rev. Metall.* **1965**, *42*, 121.
(23) Deer, W. A.; Howie, R. A.; Zussman, J. *Rock-forming Minerals, Non-Silicates*; Longmans: New York, 1962; Vol. 5.
(24) Fukasawa, T.; Iwatsuki, M.; Furukawa, M. *Anal. Chim. Acta* **1993**, *281*, 413.
(25) Crank, J. *Mathematics of Diffusion*; Oxford University Press: New York, 1956.
(26) Colombo, U.; Fagherazzi, G.; Gazzarrini, F.; Lanzavecchia, G.; Sironi, G. *Ind. Chim. Belge. Compt. Rend.* **1967**, *32*, 95.
(27) Jost, W. *Diffusion in Solids, Liquids, and Gases*; Academic Press: New York, 1952.
(28) Murad, E.; Schwertmann, U. *Clays Clay Miner.* **1993**, *41*, 111.
(29) Dieckman, R.; Mason, T. O.; Hodge, J. D.; Schmalzried, H. *Ber. Bunsen-Ges. Phys. Chem.* **1978**, *82*, 778.
(30) Huguenin, R. L. *J. Geophys. Res.* **1978**, *78*, 8481.
(31) Huguenin, R. L. *J. Geophys. Res.* **1978**, *78*, 8495.
(32) Morris, R. V.; Lauer, H. V., Jr. *Geophys. Res. Lett.* **1980**, *7*, 605.